

ASSESSMENT OF THE RISK DUE TO RELEASE OF CARBON FIBER

IN CIVIL AIRCRAFT ACCIDENTS

PHASE II REPORT

Leon S. Pocinki, Merrill E. Cornell, and Lawrence Kaplan
ORI, Inc.

SUMMARY

Under Contract NAS1-15379, ORI, Inc. investigated the risk associated with release of graphite fibers following a commercial aircraft accident and fire. The computer simulation model developed in Phase I was refined in Phase II. Additional experimental data has been made available. Phase II results indicate that the risk, considerably lower than that obtained in Phase I, is relatively small.

INTRODUCTION

This paper summarizes ORI's Phase II investigation of the risk associated with the potential use of carbon fiber composite material in commercial jet aircraft. In Phase I a simulation model was developed to generate risk profiles for several airports; the risk profiles show the probability that the cost due to accidents in any year exceeds a given amount. The computer model simulates aircraft accidents with fire, release of fibers, their downwind transport and infiltration of buildings, equipment failures, and resulting economic impact. The individual airport results were combined to yield the national risk profile. Phase II was conducted to examine the risk with more precision, and incorporate previously unavailable experimental data. These relationships are illustrated in Figure 1.

The structure of the ORI Airport Risk Model is illustrated in Figure 2. The principal steps in the simulation of each accident are illustrated in Figure 3; each is discussed in turn in this paper. The major focus is on those elements of the analysis into which changes were introduced in Phase II, principally:

- o Availability of detailed analyses of jet aircraft accidents with fire
- o Incorporation of new experimental data for the amount of carbon fiber released in a "burn"
- o Generalization of the ORI transport and diffusion model

- o New evidence indicating high filter efficiency relative to carbon fibers
- o Recent experimental values for equipment failure parameters
- o Introduction of a more detailed costing model
- o A new national risk assessment model facilitating the computation of statistical confidence limits.

The report covers these items as well as presenting brief descriptions of all other elements of the risk analysis methodology. Phase II results are compared to the previous Phase I results.

ACCIDENT WITH FIRE/RELEASE OF CF

In Phase I, ORI conducted a limited analysis of individual aircraft accident reports and summary data available through the National Transportation Safety Board. In Phase II, under NASA auspices, the major aircraft manufacturers completed a detailed analysis of approximately 100 jet aircraft accidents in which fire played a part. These analyses provided estimates of the damage to each major aircraft structural component. It was determined that the annual fire-accident rate pertinent to the risk assessment was 3.8; this has been accepted as the best estimate available for the 1993 scenario. For the risk assessment calculation we are only concerned with aircraft containing composite material, estimated to be about 70 percent of the 1993 fleet, for a resulting national mean number of carbon-fiber aircraft accidents with fire of 2.6 per year.

The calculation proceeds one aircraft size at a time. Accordingly, for airport A and aircraft of size S, we estimate the annual accident-with-fire rate by:

$$\frac{N_{A,S}}{\sum_A \sum_S N_{A,S}} \times 2.6 \quad (1)$$

where $N_{A,S}$ is the number of operations of aircraft of size S at airport A; thus the sum represents all operations in the U.S. The model computes the expression (1) from appropriate input data, and then draws a random sample from a Poisson distribution with this mean value in each replication.

In a related effort the principal aircraft manufacturers, NASA, and NASA's risk assessment contractors prepared estimates of the projected changes in the commercial aircraft fleet from now to 1993. These schedules included projected utilization of graphite fiber composite in each component. These data were combined with the accident analysis results to provide estimates of the amount of composite that would be involved in a fire following an accident to any of the projected new aircraft. In effect, for each projected aircraft type we computed the sum

$$\sum_i (\text{fraction consumed})_i \times (\text{amount of composite})_i$$

for all accidents in the airframers' analysis, where the index i refers to an aircraft component. Thus, for one aircraft type, defined by a distribution of composite material, we have the total composite that would have been consumed in each of the historical accidents. These results were then used as the probability distribution for the amount of composite involved in the fire. In each simulated accident the model determines the type of aircraft involved, based on the relative numbers of the different types in the fleet. For that type aircraft the model then draws the amount of composite involved from the distribution just described. It is then assumed that one percent of the carbon is released as 3-mm single fibers. In those accidents in which an explosion occurs, an additional two-and-a-half percent is assumed to be released due to the agitation of the composite material. These input assumptions are based on experimental evidence generated after completion of Phase I. The model also selects a random accident location based on analysis of the accident data.

PLUME

The graphite fiber release starts with an aircraft accident leading to a fire; the fire is fed by the aircraft fuel. As a result of the fire some fraction of the aircraft is consumed. The estimation of this fraction, and the ultimate amount of fiber released were discussed in the preceding section. As a consequence of the fire a hot buoyant plume is formed that rises to a "stabilization" height which is a function of the energy available, the wind speed, and the atmospheric stability. The graphite fibers enter the buoyant plume and are lifted to the stabilization height.

Plume Height Calculation

As in Phase I, calculation of the plume rise (or elevation), H , at stabilization from an open fire follows the work of Briggs (Ref. 1). The height of the plume, in meters, is given by:

$$H = 2.9 (F/us)^{1/3} \quad (2)$$

for stable conditions, and

$$H = 1.6F^{1/3} u^{-1} x^{2/3}, \text{ when } x < 3.5x^* \quad (3)$$

$$H = 1.6F^{1/3} u^{-1} (3.5x^*)^{2/3}, \text{ when } x > 3.5x^* \quad (4)$$

for neutral or unstable conditions, where u is the mean wind speed in meters per second and:

$$x^* = 14F^{5/8}, \text{ when } F < 55$$

$$x^* = 34F^{2/5}, \text{ when } F > 55$$

The buoyancy flux parameter, F, appearing in the above equations, is given by

$$F = \frac{gQ_R}{\pi C_p \rho T}$$

where:

g = acceleration of gravity, 9.8 m/sec²

Q_R = heat emission rate, kcal/sec

C_P = specific heat of air at constant pressure,
.2391 kcal/kg^oK

ρ = atmospheric density, 1.239 kg/m³

T = ambient temperature, ^oK.

The atmospheric stability parameter, s, is defined by:

$$s = \frac{g}{T} \frac{\partial \theta}{\partial z}$$

where:

$\frac{\partial \theta}{\partial z}$ = gradient of potential temperature, 0.35^o/km
for stable conditions.

Heat Emission Rate

In order to use the Briggs formulas, we must specify Q_R, the heat emission rate for a burning aircraft; this is, in turn, the product of the rate measured, gallons per unit time, and the fuel heat content per gallon. In Phase I a standard burn rate was used, based on experimental data. In Phase II we were able to turn to the detailed fire-accident analysis previously referred to. In this case it was possible to estimate the fuel burn rate for accidents occurring during different operational phases, as well as accidents of different severity. The reported accidents involved small jet aircraft almost exclusively, so a scaling factor proportional to the relative volume of the aircraft fuel tanks, as reported in Janes (Ref. 2), was used to estimate the burn rates for other size aircraft. With these inputs we are able to determine the plume rise for accidents involving different aircraft for any combination of wind speed and stability conditions.

DOWNWIND TRANSPORT AND DIFFUSION OF FIBERS

Basic Concepts

In Phase I the "standard" EPA transport and diffusion model was adapted to the needs of the risk assessment study. The model provides for downwind transport of material in the form of a plume that diffuses simultaneously in the crosswind and vertical directions. The initial source can be elevated at a specified height. The atmosphere is characterized as being in one of several stability classes. Dispersion parameters that govern the rate of crosswind and downwind diffusion are associated with each stability class (Ref. 3). The plume rise calculations, described above, give the source height, which is then used explicitly in the transport and diffusion model.

In Phase II further extensions were made to the transport and diffusion model. These allow for multiple reflections of the diffusing particles and provide an improved mechanism for accounting for particle fallout at downwind distances that are so large that the cloud is uniformly dispersed in the vertical.

The wind speed at plume height is taken as representative of the layer in which the carbon fibers are dispersing. The standard power law may be written:

$$u = u_0 (H/7)^p \quad (5)$$

The exponent p is assigned specific values for different stability classes. In most cases rather stringent physical conditions must be met for the plume to "punch through" an inversion. Observations indicate that this typically does not occur. It was therefore considered reasonable to assume that if the computed plume height is greater than the height of the inversion, it can be set equal to the inversion height.

When the vertical range over which the plume is mixed becomes equal to the depth of the mixed layer (below the inversion), we can assume a relatively uniform distribution of particles in the vertical. The model therefore makes the distribution of graphite fibers uniform in the vertical, from the ground surface to the base of the inversion, when σ_z becomes larger than $1.6 H_m$.

ORI Diffusion Equations

With these assumptions, and the Phase II modifications to allow for multiple reflections, we obtain:

$$\begin{aligned}
 D(x,y,0,H') = & \frac{Q}{\pi\sigma_y\sigma_z} \exp \left[-\frac{1}{2}\left(\frac{y}{\sigma_y}\right)^2 \right] \left\{ \exp \left[-\frac{1}{2}\left(\frac{H'}{\sigma_z}\right)^2 \right] \right. \\
 & + \text{rexp} \left[-\frac{1}{2}\left(\frac{H' + 2H_m}{\sigma_z}\right)^2 \right] + \exp \left[-\frac{1}{2}\left(\frac{-H' + 2H_m}{\sigma_z}\right)^2 \right] \\
 & + r^2 \exp \left[-\frac{1}{2}\left(\frac{H' + 4H_m}{\sigma_z}\right)^2 \right] + \text{rexp} \left[-\frac{1}{2}\left(\frac{-H' + 4H_m}{\sigma_z}\right)^2 \right] \\
 & \left. + r^2 \exp \left[-\frac{1}{2}\left(\frac{-H' + 6H_m}{\sigma_z}\right)^2 \right] \right\} \quad (6)
 \end{aligned}$$

where:

$D(x,y,0,H')$ = dosage at $x,y,0$ (receptor location) in particle-sec/m³ for the particle size of interest

x = downwind distance from source to receptor,

y = crosswind distance from source to receptor,

u = mean wind speed, m/sec,

Q = number of particles released

σ_y = standard deviation of the wind speed in the crosswind direction, as a function of x and the stability class

σ_z = standard deviation of the wind speed in the vertical, as a function of x and the stability class

r = reflection coefficient, the fraction of particles that are reflected from the ground surface

In order to incorporate the effect of particle fallout into our calculations we adopted the tilted-plume method presented by Van der Hoven (Ref. 4). Equation (6) makes use of the effective plume height, H' , given by:

$$H' = H - (v_s / u) x \quad (7)$$

At distances far enough downwind ($\sigma_z > 1.6 H_m$) that mixing results in an essentially uniform distribution of the fibers in the vertical we use:

$$D(x,y,0,H') = \frac{Q}{2.5066\sigma_y H_m u} \exp \left[-\frac{1}{2} \left(\frac{y}{\sigma_y} \right)^2 \right] \exp \left[-\frac{v_s x (1-r)}{2uH_m} \right] \quad (8)$$

Inputs to Transport Calculation

Mixing heights were developed, as in Phase I, from climatological mean values (Ref. 5) adjusted for different stability classes (Ref. 6). Sensitivity analyses are planned to test the impact of changes in mixing height values.

In many diffusion problems it is customary to determine the location of an upwind virtual point source from which a diffusing plume would have grown to the size computed for plume stabilization. In view of the large uncertainties in other phases of the risk calculation, and our concern with effects some miles downwind from the accident site, we have set the virtual point source directly over the accident/fire site.

The reflection coefficient has been set equal to 1 at the inversion and to 0.7 at the ground.

The diffusion calculation requires input values of the dispersion parameters, σ_y and σ_z , as functions of the downwind distance, x , and the prevailing stability conditions. The standard in this case is provided by the well-known Pasquill-Gifford curves. Several investigators have questioned their universal applicability; the reader is referred to Pasquill's recent work on this subject (Ref. 7). In view of the fact that no generally accepted modification of the Pasquill-Gifford curves exists, we adopted these curves for the Phase I calculations and continued to employ them in Phase II.

The basic weather inputs required - surface wind speed and direction, and stability class - are drawn from historical data. These data were obtained from the National Weather Records Center for the airports we studied; the data provide the frequency for each combination of the three weather parameters. The simulation model makes a random draw of one of these combinations weighted by the input frequency.

TRANSFER OF FIBERS INTO INTERIOR OF STRUCTURES

Method

When a building is impinged on by a plume of carbon fibers, some of the fibers may enter the building through air conditioning or other ventilation systems and by various leakage paths. Once inside the building or enclosure, fibers will be removed by fallout and through leakage paths back to the outside. If inside air is recirculated and filtered, additional fibers will be removed. The concentration of fibers that produce failure stresses on equipments in a building or enclosure at any time may be determined from equations describing the net flow. These have been developed in a relatively simple form by Slade (Ref. 4).

In Phase I, ORI was able to show that the "transfer function" or ratio of interior to exterior exposure can be expressed as:

$$\frac{E}{E_o} = \frac{v_i}{v_o + av_s + v_r} \quad (9)$$

where:

v_i = rate at which fiber-borne air enters the building, or enclosure through both the air conditioning system and through all sources of leakage

v_o = rate at which fiber-borne air leaves the building, including that removed by recirculation

v_s = fall rate of carbon fibers

v_r = rate at which fibers are removed by recirculation filtering

a = area of space subject to fallout.

Implementation

Equation (9) formed the principal basis for the calculation of interior exposure values. It was assumed that all buildings can be adequately defined by one or more of the following categories:

1. Small Equipment Building or Van
2. Medium Equipment Building
3. Large Equipment Building or Factory

4. Equipment Room inside a building
5. Utility Room
 - a) filtered
 - b) unfiltered
6. Residence
 - a) air conditioned
 - b. not air conditioned
7. Retail/Wholesale Establishments

Design factors were associated with each category of building defined above. These design factors are used to determine the air conditioning flow rates, filter efficiencies, and air leakage rates used in Equation (9). Ventilation rates were based on standards in References 8 and 9.

Phase I values of filter effectiveness were revised to incorporate Phase II experimental results. The transfer functions shown in Table I were used in all Phase II calculations. Specific building types were associated with different categories of business and industry, as described below.

EQUIPMENT FAILURES

Failure Model

The probability of failure of equipment which is exposed to carbon fibers is obtained from the exponential expression:

$$P_F = 1 - \exp(-E/\bar{E}) \quad (10)$$

where:

P_F = probability of equipment failure

E = exposure level in the immediate vicinity of the vulnerable equipment, in fiber-seconds per cubic meter

\bar{E} = average exposure causing a failure.

During Phase I, the U.S. Army Ballistics Research Laboratory (BRL) at Aberdeen, Maryland determined that experimental failure data fit an exponential failure law (Ref. 10). In Phase II it has been shown that, even for those equipments whose failures do not obey the exponential law, it is conservative to assume that the exponential law is obeyed. Typical values of the failure parameter for generic equipment types are shown in Table II.

The exposure used in Equation (10) is that directly impinging on the vulnerable equipment. When this equipment is inside a building, the interior exposure may be obtained from the exterior exposure by multiplying the exterior exposure by the appropriate transfer function (TF). Since the transfer function and the mean exposure to failure, \bar{E}_i , are constants for a particular piece of equipment in a particular building, we define a failure parameter:

$$K_{ij} = (TF)_j / \bar{E}_i \quad (11)$$

where:

K_{ij} = overall failure parameter for equipment of type i in a building of type j

$(TF)_j$ = penetration factor (transfer function) for a building of type j

\bar{E}_i = mean exposure to failure for equipment of type i.

In subsequent applications, the parameter K_{ij} is substituted into Equation (10) to give the probability of failure for equipment of type i in a building of type j for any exterior exposure:

$$P_{F,ij} = 1 - \exp(-K_{ij} E_o) \quad (12)$$

Equipment Configurations

In treating typical equipment configurations it is convenient to develop expressions for the collective probability of failure of the complete configuration. In particular, if n identical equipments are in series so that a failure of one causes the entire "line" to fail, the probability that the line fails is:

$$\begin{aligned} P_F(\text{LINE}) &= 1 - (1 - P_{F,ij})^n \\ &= 1 - e^{-nK_{ij} E_o} \end{aligned} \quad (13)$$

Similarly if n like equipments are in parallel, so that the operation fails only if all equipments fail, the aggregate probability of failure is:

$$P_F(\text{Operation}) = P_{F,ij}^n \quad (14)$$

The computer program that determines the impact of each simulated aircraft accident and associated release of graphite fibers uses Equations (12), (13), (14) to

estimate the probability that each business or industry in the geographical area of interest is affected.

One of the major efforts in Phase I was the characterization of each business-industry sector, defined by an SIC (Standard Industrial Classification) number, by a specific set of equipments installed in a specific building. This effort was extended and made more detailed in Phase II. A complete basic equipment configuration is shown in Figure 4; in any particular facility one or more portions of this configuration may not be present. In addition, the equipment "suit" is made specific to plant size (small, medium, or large). An example will illustrate the method. A large plant in Category 28A (comprising all 3-digit SIC code numbers under 28, basically chemical and allied products) has an internal power interface characterized by one set of input power service equipment, one distribution panel, and auxiliary power equipment. Its common module consists of two computers in parallel and two keyboard display units in parallel. The plant has 25 lines in its distributed module. Each line consists of:

- o 5 high-voltage power supply units
- o 5 interface units
- o 5 manual controllers
- o 5 minicomputers, used as controllers
- o 2 high-voltage motor controllers
- o 2 machine station servo-mechanisms
- o 1 heater control unit
- o 5 sensor units.

Similar configurations were defined for all vulnerable categories of business and industry. The data was developed as a result of an extensive literature search, augmented by site visits during Phases I and II. The different building types defined in Table I are related to the different modules of each type of vulnerable business and industry. For example, Table III associates the different building types with the major sections (modules) of plants of different size in Category 28A.

Computer Implementation

The mean exposure-to-failure values for several of the generic equipments defined above are summarized in Table II. In using these inputs the equipment-specific value of \bar{E} was combined with the building-specific transfer function, in accordance with Equation (11). In order to estimate the impact on specific business and industrial complexes it was assumed that the plant is down if electric power is lost inside the plant, if the common module fails, or

if more than one half of the "lines" in the distributed module fail. Since Phase II results reported by other investigators indicated that the high-voltage power supply system is essentially invulnerable, it was assumed that an equivalent piece of equipment representing the output bushings and buss of a step-down transformer could be used to represent the possibility of an exterior power supply failure.

COSTS ASSOCIATED WITH EQUIPMENT FAILURES

Scope of Calculation

This section of the paper presents ORI's Phase II methodology for determining the costs associated with equipment failures. The most significant changes to the Phase I methodology were introduced in this part of the risk assessment calculation. Three categories of cost were defined for business and industry impacts:

- o Repair of damaged electrical equipment
- o Facility cleanup
- o Business/industry disruption.

In the Phase I risk assessment, attention was focussed on the latter cost category using an expected value technique. In Phase II the model has been expanded to treat all the above categories explicitly, while disruption costs are now computed by a Monte Carlo process. Household equipment failures are treated as in Phase I. A completely new module has been introduced to compute the cost incurred due to repair of damaged avionics equipment.

Repair Costs

A repair cost was defined for each generic type of equipment shown in Table II. Categories of business and industry were defined by SIC code (primarily at the three-digit level) as well as by size. As described in the preceding section each facility has a specific number of each equipment type. The model computes the probability of failure for each type of equipment at a particular location; the number that fail is determined in a Monte Carlo random draw. Model inputs include the equipment repair costs. The product of the number that fail and the repair cost yields the repair costs associated with that kind of equipment at that location.

Facility Clean-Up Costs

Estimates of facility clean up costs were made for different businesses and industries on the basis of type of business and size of plant. Using information gained during the Phase II site visits it was estimated that the decision to institute a special plant-wide clean up would be made on the basis of evidence of major impact of the presence of carbon fibers. Accordingly, it is assumed that an intensive plant cleanup is implemented whenever the plant is shut down due to equipment failures, as described below.

Dislocation Cost

It was assumed that a plant or place of business would be shut down if power is lost, the common module fails, or more than half of the production lines fail. This determination is made for each plant in one SIC-code group at the location. In contrast to Phase I, then, we determined plant closings on a plant-by-plant basis, rather than employing an expected-value algorithm.

The fraction of an industry or business shut down was estimated by computing the employee-weighted fraction of production lost. The method may be expressed as:

$$F.C._{SIC} = \frac{\sum_{Size} (No. of Empl.)_{SIC, Size} \times (No. of Plants Shut)_{SIC, Size}}{\sum_{Size} (No. of Empl.)_{SIC, Size} \times (No. of Plants)_{SIC, Size}} \quad (15)$$

The risk assessment model assumes that the impact of a carbon fiber incident on the economy can be measured by the fraction of the local GDP allocated to a particular industry over the period of time that the industry is "down." We assumed that the down time would be of the order of one day. The impact in dollars is then calculated by using this result in the following algorithm:

$$Cost = K \sum_{SIC} \frac{(Local Payroll)_{SIC}}{(National Payroll)_{SIC}} GDP_{SIC}^{FC} \quad (16)$$

National-level inputs from the Department of Commerce provide the national payroll broken out by SIC number and the Gross Domestic Product broken out by SIC number. Available data for counties surrounding the particular airport include payroll for each SIC-coded business and industry. The factor K adjusts the result for the fraction of a year the plant remains shut, since the other data is typically annual.

Household Impact

The method used in Phase II is essentially the same as that employed in Phase I. We define the fraction of households in an area that are air conditioned (FAC) and use the methods previously described to estimate the failure probability of vulnerable equipment in air conditioned and non-air conditioned households. The latter calculation includes both the failure and ventilation parameters. If the resulting failure probabilities are $P_{F,AC}$ in the air conditioned household and $P_{F,NAC}$ in the non-air conditioned household, then the

estimated cost to repair all damaged equipments of a particular class at all households is given by:

$$\text{Repair Cost} \times \text{Number of Households} \times \text{Number of Equipments per Household} (P_{F,AC}^{\text{FAC}} + P_{F,NAC} (1 - \text{FAC}))$$

The locations and numbers of residential units were obtained from the Bureau of Census publication, County and City Data Book. Based on the latest experimental evidence our attention was limited to household television and high fidelity equipment, while updated Phase II ventilation data were used.

Geographical Area Specification

As in Phase I, county-based economic data was adopted for computer input; in many cases counties were divided into smaller, homogeneous geographical units. In each case the center of the county or sub-county geographical unit was selected and a representative circle inscribed within the area. The input data set includes the coordinates of the center and the associated radius. The exposure and resulting impact calculations are made at the center and points a distance equal to two-thirds of the radius to the east, west, north, and south of the center. In each case the county-based business/industry sites are uniformly distributed over these five points. The concept is illustrated schematically in Figure 5, as applied to one county for the Washington National Airport risk calculations. In all cases this method was applied to the area around each airport to a distance of 80 km or more.

Aircraft Vulnerability

In Phase I, ORI concluded that key airport operations were relatively invulnerable due to the many designed redundancies in the system. The analysis did not cover the risk to aircraft on the ground at the time of the accident. Because of safety-of-flight, as well as other factors, it was decided that an investigation should be made of the risk to aircraft on the ground, at passenger gates and maintenance locations. This was initiated in Phase II, and focussed on failures of avionics equipment. In a cooperative effort the aircraft manufacturers analyzed data to determine the number of aircraft expected to be at passenger boarding gates and at maintenance locations on the airport by day and night. This was done for the nine airports previously selected as representative (with a bias toward the busier airports). The 1978 data were extrapolated to the 1993 time frame, based on estimated fleet changes. For aircraft at each location a survey was made to provide estimates of the fraction of time each aircraft is in each of several defined ventilation modes. Transfer functions were estimated for each of these ventilation modes, for each of several locations on board small, medium, and large aircraft. The latter data, together with mean-exposure-to-failure values for typical avionics equipment enabled us to estimate the probability of failure of each of several generic classes of avionics equipment on board each aircraft.

A summary of key avionics equipment input data is shown in Table IV. The

aircraft vulnerability module first randomly determines whether the accident occurred during day or night; it then selects the number of each size aircraft at representative gate and maintenance locations. The model aggregates each type of vulnerable equipment over all aircraft in one size range, and randomly determines, based on the input probabilities, the number of equipments in that category in each ventilation mode (transfer function value). The model computes failure probabilities and randomly determines the number of equipments that fail for the computed exterior exposure at each location. With the input repair costs we then determine the total cost. These steps are illustrated in the flow chart appearing as Figure 6.

Costing Summary

At one geographical location the model computes business-industry impact as the sum of costs of equipment repair, facility cleanup, and business disruption. At those locations defined as residential centers the model computes the total cost due to household equipment failures. At the airport the model computes costs required to repair failed avionics equipment. Summary results for each simulated accident present the total of costs in each of these three major categories, obtained by adding the costs over all geographical locations that were affected by the accident.

RESULTS OF AIRPORT SIMULATIONS

Basic Results

The simulation model was run for the nine airports previously studied in Phase I, and listed below:

O'Hare/Chicago

John F. Kennedy/New York City

Washington National Airport/Washington, D.C.

Lambert/St. Louis

LaGuardia/New York City

Logan/Boston

Hartsfield/Atlanta

Miami International/Miami

Philadelphia International/Philadelphia.

Figure 7 illustrates, schematically, the results provided by the simulation of randomly selected accidents. The data for one sample accident is shown in Figure 8. Randomly selected accident and weather parameters are indicated.

In this accident all impacts were limited to Queens County, represented by the circle, where the average exposure was 3.5×10^4 fiber-seconds per cubic meter. Damage to households there totalled \$533; business impact was \$37,177, of which \$5,600 was equipment repair cost and \$31,577 was due to business closings.

For each airport the number of samples (replications) was selected so that at least 2500 accidents were simulated. In this section of the paper several examples of the results are presented. The accident results are summarized in Table V. The table shows that the airports near relatively small centers of population tend to have somewhat less costly accidents. The damage to avionics equipment appears to be small at all airports; the largest single impact on avionics in all simulated accidents was \$3,910 at Kennedy Airport.

Risk profiles were computed for all of the airports. Examples of several are shown in Figure 9. We first note that O'Hare/Chicago, the nation's busiest airport has a risk profile that shows that the probability of exceeding \$10,000 in total CF-related impact is approximately .0004. For St. Louis, the corresponding probability is approximately .0001 (one in 10,000). In comparing the risk profiles shown in Figure 9, it should be noted that O'Hare Airport is a high traffic airport serving a major urban area; Atlanta's airport is also one of the busiest in the nation, while its population concentration is somewhat smaller. St. Louis is characterized as both a low-traffic airport and a relatively low population concentration.

Accuracy/Sensitivity Test Results

Several special analyses were conducted. We computed statistical confidence limits for the risk profiles. In Phase I it was shown that the 95% confidence limits could be expressed as:

$$p \pm 2 \sqrt{\frac{p(1-p)}{n}}$$

where p is the computed exceedance probability after simulating n samples. Figure 10 shows the Washington National Airport risk profile with the 95% confidence limits. The confidence limits apply to the purely statistical nature of the simulation, and not to the impact of errors in input data. The results do show that conclusions based on the risk profiles need not be altered because of inherent statistical uncertainty.

An example of sensitivity testing that can be conducted with the ORI risk assessment model is shown in Figure 11. In this figure, two O'Hare/Chicago risk profiles are compared: the best estimate in which the mean amount of composite per aircraft is 2803 kilograms, and a "worst case" in which all aircraft operating at O'Hare are assumed to be large jets with the maximum composite considered for any aircraft, 15,600 kilograms. The comparison shows the significant impact of the increased carbon fiber. Even in this case, however, the probability of exceeding \$10,000 in annual damages is only about .005 (five in a thousand).

To test the effect of increasing the sample size the O'Hare/Chicago simulations were run for 22,000 and 44,000 annual samples, resulting in 2537 and 5038 accidents respectively. The outputs are compared in Table VI. The 44,000-sample case indicates that a significantly larger extreme value occurred. The risk profile results are, however, quite similar.

NATIONAL RISK

Method

In order to estimate the total national risk the set of airports for which the individual risk profiles were obtained was used to represent the entire United States. This set of airports accounts for approximately one-third of the nation's commercial traffic. Since they are predominately large, busy airports, this method overestimates the national risk. A random number of accidents is generated for a one-year replication at the national level. Individual accidents are allocated to airports on the basis of that airport's share of the total traffic. Instead of "replaying" the simulation for each airport we saved the individual accident results from the single airport simulations. For each airport that an accident is allocated to, the national model draws an accident at random from that airport's accidents that were simulated previously. Figure 12 is a flow chart for this calculation.

Results

The results of the calculation, using results from the individual airports, and the weighting factors described above, indicate a maximum annual impact for business and industry of \$274,000, with a mean of \$466. For avionics impact the results are \$3,900 and \$2, respectively. The national risk profile with the 95% statistical confidence limits is shown in Figure 13. In Figure 14 the Phase I and Phase II results are compared, showing that the new Phase II inputs result in a greatly reduced estimated risk.

SUMMARY AND CONCLUSIONS

ORI, Inc. has developed a versatile generally applicable risk assessment simulation model. Using the best available data - we have assessed the risk associated with the use of carbon fiber composite material in commercial aircraft. Confidence in model-generated results is relatively high, based on examination of the statistical confidence limits, model stability, and sensitivity tests. As a result we conclude that the use of carbon fiber composite material in commercial aircraft structures constitutes a relatively low risk.

REFERENCES

1. Briggs, G.A.: "Some Recent Analyses of Plume Rise Observations." Paper presented at the 1970 International Air Pollution Conference of the International Union of Air Pollution Prevention Associations.
2. Janes All The Worlds Aircraft.
3. User's Manual for Single-Source (CRSTER) Model, EPA, July 1977, EPA-450/2-77-013.
4. Meteorology and Atomic Energy 1968, David H. Slade, Editor, AEC, July 1968.
5. George Holzworth, Mixing Heights, Wind Speeds, and Potential for Urban Air Pollution Throughout the Contiguous United States, EPA, January 1972.
6. K. L. Calder, "A Climatological Model for Multiple Source Urban Air Pollution, Appendix D" to A. D. Buse and J. R. Zimmerman, User's Guide for the Climatological Dispersion Model, EPA-73-024, December 1973.
7. Pasquill, F., Atmospheric Dispersion Parameters in Gaussian Plume Modeling, Part II, "Possible Requirements for Change in the Turner Workbook Values," EPA, Research Triangle Park, June 1976, EPA-600/4-76-0306.
8. Carrier Air Conditioning Co., Handbook of Air Conditioning System Design, McGraw-Hill Book Co., 1965.
9. Standard Handbook for Mechanical Engineers, Baumeister & Marks, McGraw-Hill, 1967.
10. Have Name Vulnerability of the Improved Hawk System, BRL Report No. 1964, Shelton and Moore, February 1977.

TABLE I. - VALUES OF TRANSFER FUNCTION FOR TYPICAL ENCLOSURES

Enclosure Category	Transfer Function
1. Small Equipment Building or Van	.012
2. Medium Equipment Building	.010
3. Large Equipment Building or Factory Building (per floor)	.004
4. Equipment Room in Building (one exterior wall)	.010
5. Utility Room	Filtered .023
	Non-Filtered .094
6. Residence	Air Conditioned .058
	Non-air Conditioned .004
7. Retail/Wholesale Establishment	.004

TABLE II. - MEAN EXPOSURE TO FAILURE (\bar{E}) FOR TYPICAL GENERIC EQUIPMENTS
(Fiber-Seconds per Cubic Meter)

<u>Equipment</u>	<u>\bar{E}</u>
High-voltage Power Supply	10^8
Interface Unit	10^8
Manual Controller	10^8
Computer ("Standard Size")	10^7
Keyboard-Display Unit	10^8
High-voltage Motor Controller	10^8
Machine Station Servo-Controller	10^8
Sensor	10^7
Power Distribution Panel	10^8
Switchgear	10^8
Auxiliary Generator	10^6

TABLE III. - ASSOCIATION OF PARTICULAR BUILDING TYPES*
 WITH INDUSTRIAL FACILITY FOR SIC 28 - CHEMICAL
 AND ALLIED PRODUCTS

Plant Size	POWER MODULE			COMMON MODULE	DISTRIBUTED MODULE
	SW	DIST.	AUX.		
Large	5b	3	5b	4	3
Medium	5b	3	-	-	3
Small	5b	2	-	-	2

* SEE TABLE I

TABLE IV. - AIRCRAFT AVIONICS EQUIPMENT CONFIGURATIONS WITH FAILURE AND COST INPUTS

Aircraft Size	Avionics Equipment ID No.	Number on Aircraft	\bar{E} (Failure Parameter*)	Repair Cost (\$)
Small	1	38	10^8	100
	2	7	1.5×10^7	100
	3	6	10^8	450
	4	2	1.5×10^7	450
	5	1	10^8	300
	6	18	10^8	50
Medium & Large	7	26	1.5×10^7	215
	8	24	10^8	220
	9	153	10^8	175
	10	4	10^8	250
	11	22	10^8	210
	12	43	10^8	385
	13	3	10^8	530
	14	2	10^8	1295
	15	4	10^8	1665

*In fiber-seconds per cubic meter.

TABLE V. - RESULTS FOR SIMULATED ACCIDENTS AT NINE AIRPORTS (1976 DOLLARS)

Airport	Mean			Avionics	Mean of 10 Worst
	Household	Bus/Ind.			
Atlanta	1	70		2	14,238
Boston	2	152		0	35,818
Wash. Nat'l.	5	310		0	62,497
Kennedy	11	199		3	32,544
LaGuardia	11	373		0	56,186
Miami	2	28		1	7,566
Chicago	6	162		1	32,510
Philadelphia	7	192		0	28,971
St. Louis	2	67		0	13,779

NOTE: Approximately 2500 accidents simulated for each airport.

TABLE VI. - 1993 CHICAGO/O'HARE COMPARISON OF DIFFERENT SETS OF SIMULATIONS

	22,000 Samples	44,000 Samples
No. of Accidents	2537	5038
Mean Accident	\$147	\$166
Worst Accident	\$54,000	\$110,299
$P > \$1,000$.000955	.00111
$P > \$10,000$.000545	.000545

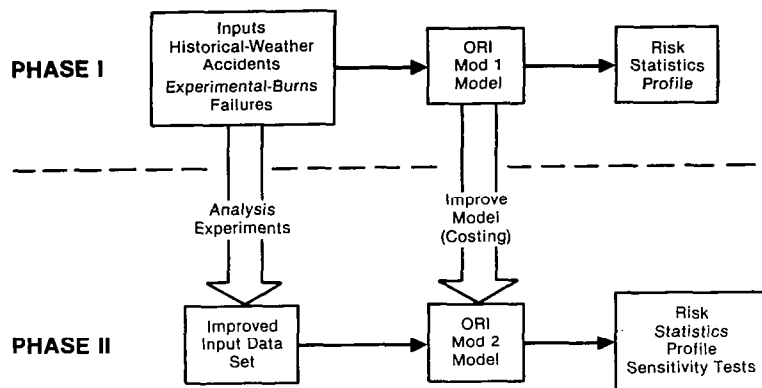


Figure 1.- Conceptual relationship of Phases I and II - ORI carbon fiber risk assessment program.

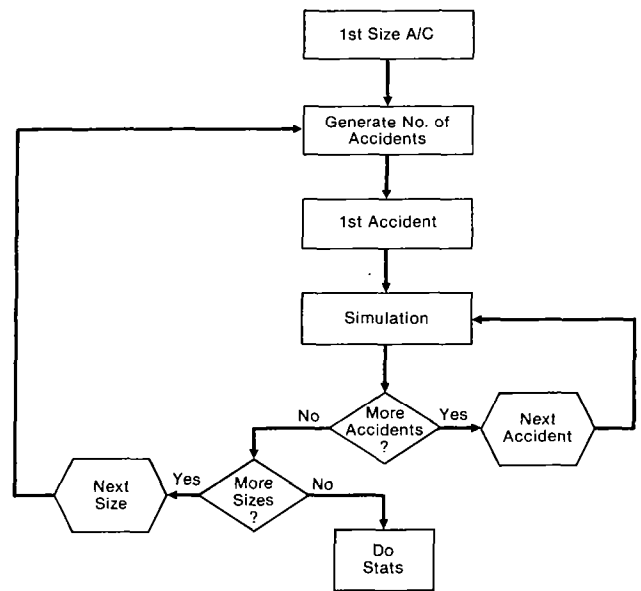


Figure 2.- Flow chart for ORI airport risk model.

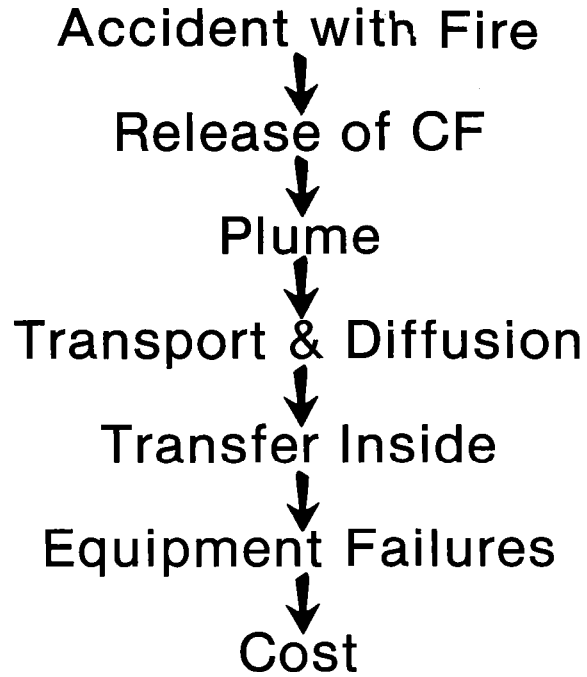


Figure 3.- Events in aircraft accident scenario replicated in each accident simulation.

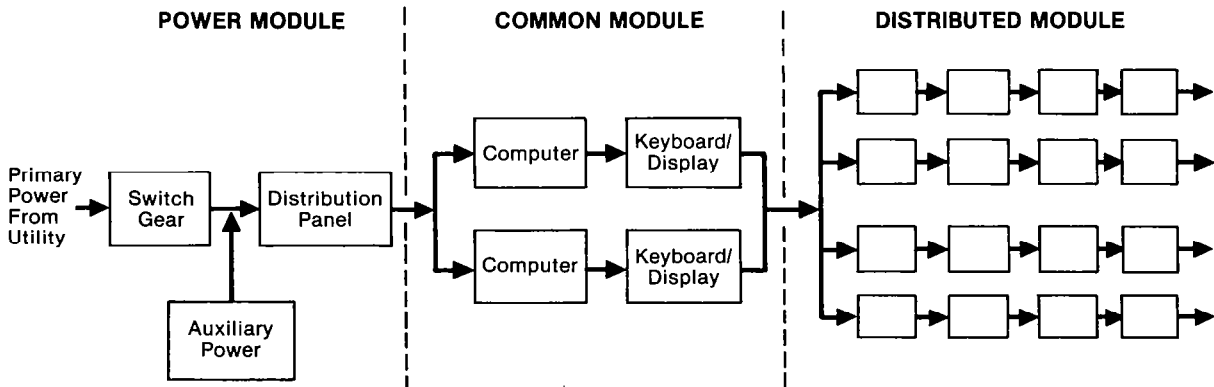


Figure 4.- Schematic electric power flow in typical business/industry facility.

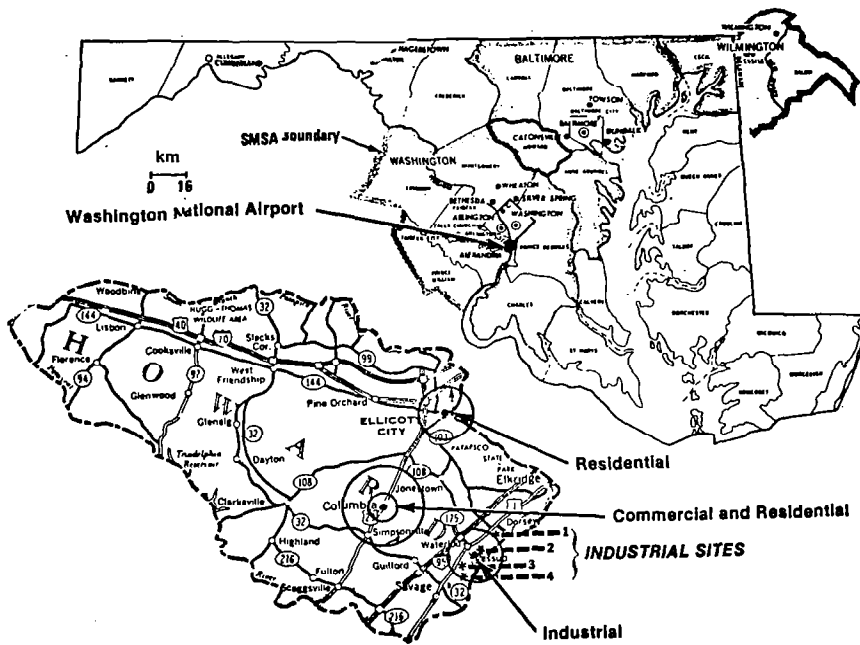


Figure 5.- Definition of areas at risk for Washington National Airport. Howard County, Maryland, outlined in upper map, shown in detail in lower map. Circles represent concentrations of business, industry, and residences.

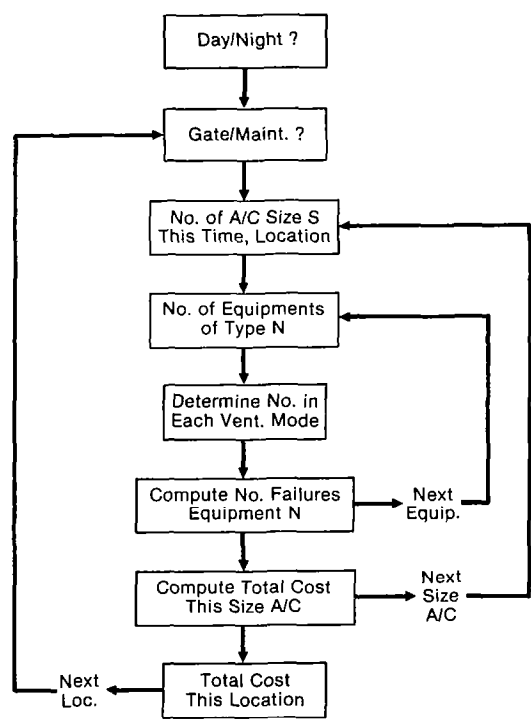


Figure 6.- Flow chart for modeling avionics equipment failures.

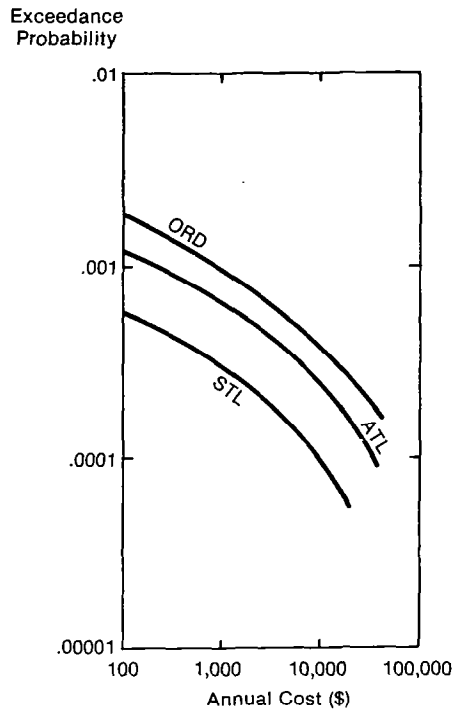


Figure 9.- 1993 risk profiles for selected airports. ORD is O'Hare/Chicago; ATL is Hartsfield/Atlanta; STL is Lambert/St. Louis.

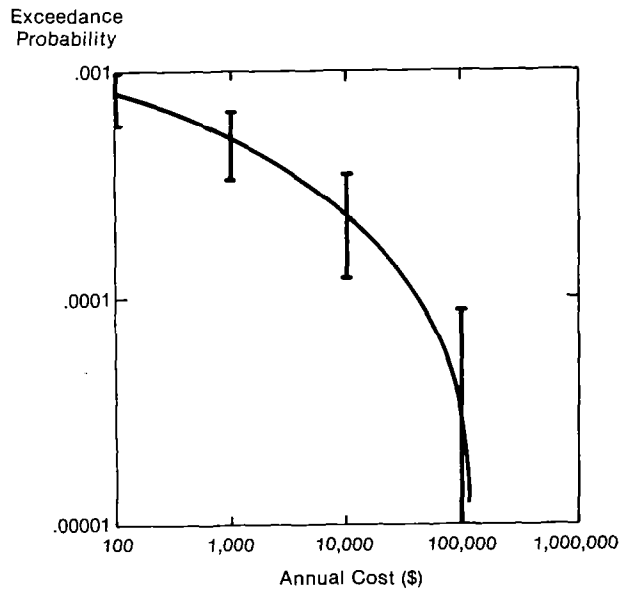


Figure 10.- 1993 risk profile for Washington National Airport with 95 percent statistical confidence limits.

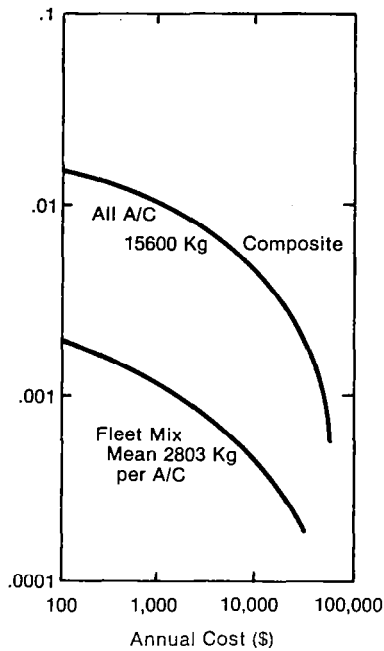


Figure 11.- 1993 risk profiles for O'Hare/Chicago. Comparison of best-estimate with "worst case" in which all aircraft are large jets with maximum carbon fiber.

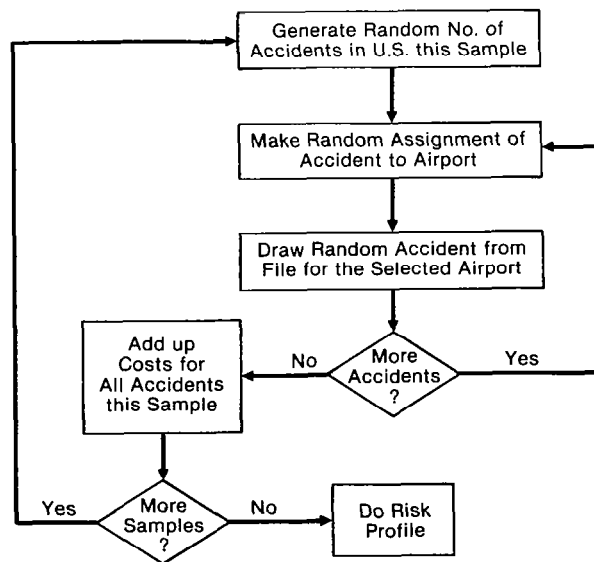


Figure 12.- Flow chart for computing national risk.

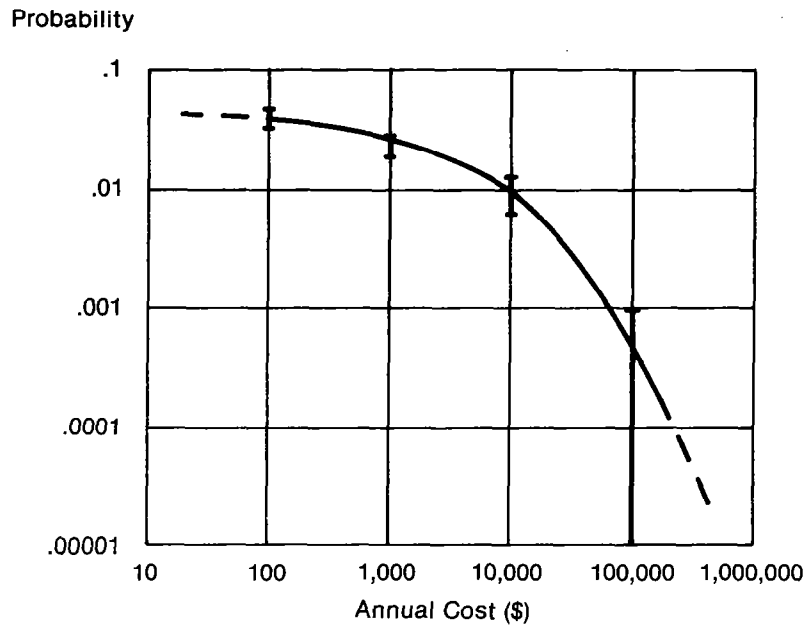


Figure 13.- 1993 national risk profile with 95 percent statistical confidence limits.

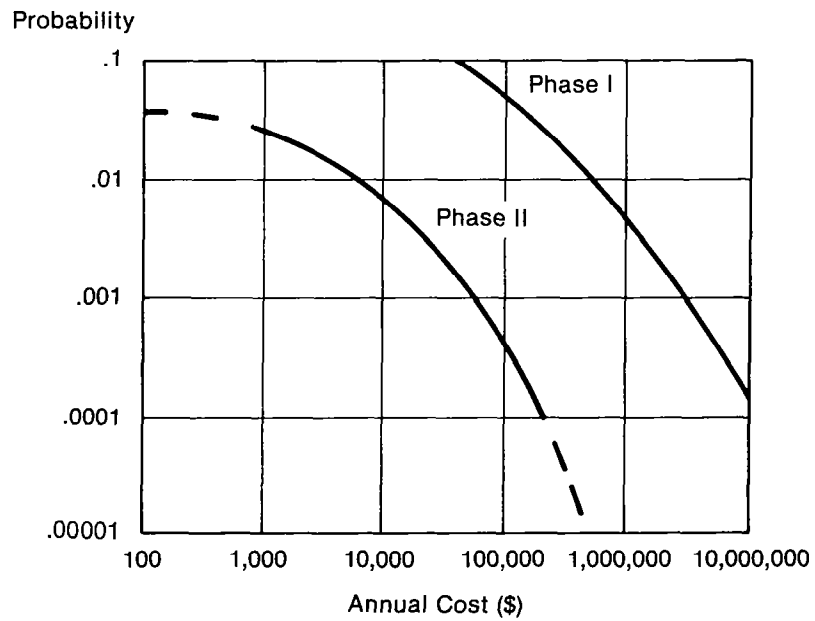


Figure 14.- Comparison of Phase I and II national risk profiles.